



Integrated dataset of atmospheric bioaerosols over east Asia

Zhongwei Huang^{1,2}, Wenjin Zhang¹, Qing Dong¹, Teruya Maki³, Yongkai Wang¹, Yuanzong Ji¹, Fanli Xue¹, Xuefei Huo¹, Da Lu¹, Dongdong Wang¹, Jinsen Shi^{1,2}, Jianrong Bi^{1,2}, and Jianping Huang^{1,2}

¹Key Laboratory of Semi-Arid Climate Changes with the Ministry of Education, College of Atmospheric Sciences, Lanzhou University, Lanzhou, 730000, China

²Collaborative Innovation Center for Western Ecological Safety, Lanzhou University, Lanzhou, 730000, China

³Department of Life Science, Faculty of Science and Engineering, Kindai University, Higashiosaka, Osaka, Japan

Correspondence to: Jianping Huang (hjp@lzu.edu.cn)

Abstract. Bioaerosols are one of the main types of aerosols originating from the Earth's biosphere and are widely found in the atmosphere. They possess both biological attributes and aerosol characteristics, thereby exerting significant influences on climate, the environment, ecosystems, and public health. However, their regional-scale distribution, influencing factors, climatic and environmental impacts remain unclear due to the scarcity of observational data. This study firstly establishes an integrated bioaerosol dataset based on a large-scale dust–bioaerosol field campaign conducted across East Asia using unified sampling and analytical methods. The dataset systematically integrates atmospheric bioaerosol number concentrations and bacterial community structure at multiple taxonomic levels across 45 sites in China, Japan, South Korea, and Mongolia. In addition, meteorological variables (e.g., air temperature, relative humidity, wind speed and direction), air quality parameters (e.g., PM₁₀ and PM_{2.5}), and Normalized Difference Vegetation Index (NDVI) data during the sampling period were incorporated from multiple sources. Further analysis of this integrated dataset indicates that bioaerosol number concentrations are negatively correlated with local NDVI. Moreover, there is a clear relationship between bioaerosol number concentration and air temperature, with a peak observed at approximately 10–15 °C. A pronounced diurnal variation in bioaerosol concentrations is also found, which is strongly associated with Aerosol Optical Depth (AOD) and particulate matter concentrations. In addition, substantial differences in community structure were observed across different underlying surface types, and the α -diversity indices (Shannon and Chao1 indices) were negatively correlated with NDVI. This dataset provides a robust foundation for advancing research on atmospheric bioaerosol processes, as well as their implications for climate, the environment, public health, and interdisciplinary studies. The dataset generated in this study is openly available via Zenodo (<https://zenodo.org/records/19605145>)(Huang et al., 2026).

1 Introduction

Bioaerosols are defined as living aerosol particles, biologically active components, and metabolic products of organisms, with particle diameters ranging from 0.001 to 100 μm (Fröhlich-Nowoisky et al., 2016; Després et al., 2012). For coarse-mode particles with diameters greater than 1 μm , these particles typically account for approximately 30% of both number and mass



concentrations in urban and rural atmospheres, and their contribution can reach up to 80% in pristine rainforest regions (Fröhlich-Nowoisky et al., 2016). Bioaerosols are transported through the air, due to their small size and low density, can be readily dispersed across different environments (Van Leuken et al., 2016). Because they exhibit both physical and biological properties, they play important roles in public health, climate processes, and ecosystem functioning (Du et al., 2018; Huang et al., 2024a).

Most bioaerosols fall within the respirable size range (Bulski, 2020; Estillore et al., 2016), which allows their entry into the human body via the respiratory tract or penetrate compromised skin and mucous membranes, thereby posing potential health risks (Bulski, 2020). Deposition in different depths within the respiratory system may induce allergic or toxic responses in both humans and animals (Hofmann, 2011; Eriksen et al., 2023). Bioaerosols also play critical roles in modulating climate change. As airborne particulate matter, they absorb and scatter solar and terrestrial longwave radiation, thereby exerting direct regional and global radiative forcing (Huang et al., 2024a). Furthermore, bioaerosols can act as nuclei for cloud condensation, ice crystals, and precipitation, thereby influencing hydrological cycles and climate systems (Fröhlich-Nowoisky et al., 2016; Huang et al., 2025). A unique property of airborne biological components is their ability to produce ice-nucleating proteins (INPs), which can promote ice developing when subzero temperatures are relatively high (Hoose and Möhler, 2012). These biological INPs are active above -15°C , whereas mineral dust particles typically are not (Morris et al., 2013). In addition, atmospheric microorganisms can influence the photochemical and chemical reactions of aerosols, thereby altering their composition (Péguilhan et al., 2025), with consequent feedbacks on climate processes (Meinander et al., 2022). Both viable and inactivated microbial cells exhibit comparable oxidative potential and may even enhance the oxidizing power of chemical species in the atmosphere (Samake et al., 2017).

Bioaerosol sampling has been conducted worldwide, yielding data on their distribution, composition, sources, and atmospheric roles, thereby advancing our understanding of their behavior and influencing factors (Huang et al., 2024b; Zhang et al., 2022b; Petersson Sjögren et al., 2023; Jabeen et al., 2023). However, existing studies lack standardized sampling and analytical protocols. Even when operated simultaneously, different sampling instruments may produce varying bioaerosol signals and exhibit differences in collection efficiency for different types of microorganisms (Mainelis, 2019; Mescioglu et al., 2021; Mbareche et al., 2018). The pore size and material of filter membranes can influence results of airborne microbiome studies (Guo et al., 2024; Jeong and Kim, 2021). Differences in sampling flow rate can also affect results, as high flow rates increase the risk of adverse effects (Boifot et al., 2024). Following collection, temperature conditions during sample transport and short- or long-term storage, can influence DNA degradation and alter sample composition (Clasen et al., 2020). These factors collectively reduce sample comparability and affect downstream analyses. During molecular analysis, significant differences in taxonomic richness, community composition, and diversity may arise from the selection of different 16S rRNA variable regions (Larsen et al., 2015; Lin and Ju, 2023). The application of different reference databases for taxonomic classification can also yield divergent results due to inherent database discrepancies (Balvočiūtė and Huson, 2017; Ramakodi, 2022). Together, these factors complicate cross-study comparisons. Although many studies aim to link environmental, meteorological, and chemical factors with bioaerosols, variations in sampling and analytical methods may lead to contradictory conclusions



65 and hinder the development of robust findings, as it is often unclear whether discrepancies arise from environmental variability or methodological heterogeneity (Sajjad et al., 2023; Mainelis, 2019; Pogner et al., 2024).

At present, the spatial and temporal coverage of bioaerosol sampling remains sparse (Zawadowicz et al., 2019). Many observations are restricted to isolated field campaigns or single-site stations, with particularly limited coverage in arid regions and developing countries (Shammi et al., 2021). In addition, long-term continuous records are scarce, and standardized time series spanning multiple years and sites are largely lacking. This limitation not only constrains the detection of long-term trends and interannual variability but also hampers the use of observations for model calibration and the assessment of climate-scale impacts (Huang et al., 2024a; Safatov et al., 2022). Furthermore, methodological heterogeneity across studies complicates data integration and limits large-scale analyses (Alfaro-Perez et al., 2025). Given the highly dynamic nature of the atmosphere, bioaerosol concentrations exhibit substantial spatial and temporal variability (Šantl-Temkiv et al., 2019), and conclusions derived from studies with limited spatial or temporal coverage may therefore be inconsistent (Jiang et al., 2022). Together, these factors further reduce the robustness of integrated assessments of bioaerosol impacts on climate, the environment, ecosystems, and human health (Gashi et al., 2025).

To accurately quantify bioaerosol-related effects, there is an urgent need to expand observational network coverage, establish long-term continuous monitoring records, and advance methodological standardization to enable regional and transregional data integration and sharing (Huang et al., 2024a). Therefore, establishing a bioaerosol dataset with broad geographic coverage and unified sampling and analytical methodologies is of great importance for advancing scientific research and applications (Sajjad et al., 2023; Gashi et al., 2025; Boifot et al., 2024; Jiang et al., 2022). Such a dataset would enable improved characterization of the geographic distribution, spatiotemporal variability, and environmental and health impacts of bioaerosols. Under ongoing climate change, drought conditions are projected to intensify (Araujo et al., 2025; Xu et al., 2023), with East Asia expected to be strongly affected (Qi et al., 2024). Dust generated during sandstorm can promote the long-range transport of bioaerosols (Maki et al., 2019; Zhou et al., 2024). Considering the extensive arid and semi-arid regions of East Asia and the large populations residing downwind (Yu et al., 2023; Jin et al., 2022), the potential risks associated with bioaerosols in this region are relatively high. Establishing such a dataset will support improved assessment of public health risks under climate change and provide a scientific basis for mitigation and policy development.

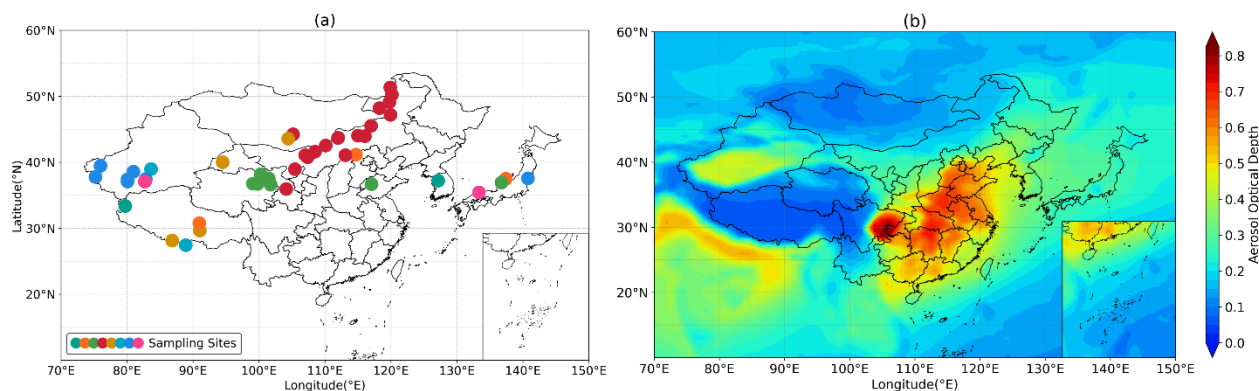
90 **2 Sampling sites and methods**

2.1 Sampling sites

The DuBi (Dust–Bioaerosol) field sampling campaign was conducted over an extended period and across a broad spatial domain. From 2011 to 2021, sampling was performed at multiple sites across East Asia, including China, Japan, South Korea, and Mongolia (see Table 1 for details). These sites encompass a wide range of surface types and climatic conditions, providing strong regional representativeness and ensuring comparability among observations (Fig. 1).



This field observation campaign substantially enhanced the temporal and spatial coverage of bioaerosol measurements in East Asia. As a result, the compiled dataset enables a more comprehensive characterization of bioaerosol distributions across diverse environmental settings, thereby improving our understanding of the regional features and evolution patterns of bioaerosols in East Asia.



100

Figure 1: (a) Spatial distribution of sampling sites from 2011 to 2021; (b) spatial distribution of the mean aerosol optical depth (AOD) from 2000 to 2020.

Table 1: Summary of land surface characteristics, number of samples, locations, sampling period (local standard time, LST), and sampling duration throughout the DuBi field campaign conducted between 2011 and 2021.

Sampling Site	Land Surface	number of samples	Latitude & Longitude	Sampling Period	Sampling Duration
Dunhuang	-	13	(94.5° E, 40.1° N)	2011/9/9-2011/9/10 2021/7/11-2021/7/19	1-12h
Kanazawa	-	47	(136.7° E, 36.5° N)	2011/3/22-2011/5/1 2017/4/21-2017/5/15 2017/9/5-2017/9/28	6-15h
Hakui	-	2	(136.8° E, 36.9° N)	2013/4/28 2014/3/28	1h
Tsogt-Ovoo	-	14	(105.2° E, 44.2° N)	2014/3/16-2014/3/18 2017/4/29-2017/5/4	2-18h
Namie	-	59	(140.8° E, 37.6° N)	2015/8/19-2018/3/22	-
Erlianhot	Sandy land	111	(111.9° E, 43.7° N)	2016/3/30-2016/5/25 2017/8/17-2017/8/19	2-24h
Zhangbei	Sparse grassland	140	(114.7° E, 41.2° N)	2016/3/29-2016/5/31	2-15h
Jinan	Urban	121	(117.1° E, 36.7° N)	2016/3/23-2016/6/4	7-34h



Dalanzadgad	Road	5	(104.4° E, 43.6° N)	2017/5/1-2017/5/3	-
Bayannur	Urban	2	(107.4° E, 40.8° N)	2017/8/4	3-6h
Ulanqab	Sparse grassland	2	(113.1° E, 41.1° N)	2017/8/4-2017/8/5	3-8h
Xilinhot	Urban	1	(116.1° E, 44.0° N)	2017/8/5-2017/8/6	8h
Arxan	Urban	4	(119.9° E, 47.2° N)	2017/8/6-2017/8/7 2017/8/14	3-9h
Ewenki Autonomous Banner	Urban	7	(119.8° E, 49.1° N)	2017/8/7-2017/8/8	4-11h
Ergun	Urban	3	(119.9° E, 51.3° N)	2017/8/9-2017/8/10	3-9h
Labudalin	Wetland	2	(120.1° E, 50.2° N)	2017/8/10-2017/8/11	4-10h
New Barag Left Banner	Sparse grassland	3	(118.3° E, 48.2° N)	2017/8/13-2017/8/14	4-9h
East Ujimqin Banner	Sparse grassland	2	(117.0° E, 45.5° N)	2017/8/15-2017/8/16	4-9h
Abag Banner	Sparse grassland	2	(115.0° E, 44.0° N)	2017/8/16-2017/8/17	4-9h
Baotou	Sparse grassland	2	(110.1° E, 42.5° N)	2017/8/19-2017/8/20	4-11h
Urad Middle Banner	Sparse grassland	2	(108.5° E, 41.6° N)	2017/8/20-2017/8/21	4-9h
Urad Rear Banner	River dam	2	(107.0° E, 41.1° N)	2017/8/21-2017/8/22	4-11h
Alxa Left Banner	Grassland	2	(105.5° E, 38.9° N)	2017/8/22-2017/8/23	4-10h
Yongjin	-	68	(127.16° E, 37.2° N)	2018/3/9-2018/7/4	-
Lhasa	-	11	(91.0° E, 29.6° N)	2018/5/7-2018/5/8 2018/5/27-2018/5/31	9-13h
Everest Base Camp, Xigaze	-	28	(86.9° E, 28.1° N)	2018/5/11-2018/5/24	7-14h
Tazhong	Desert	40	(83.7° E, 39.0° N)	2019/7/7-2019/7/30	9-22h
Minfeng	Grassland	31	(82.7° E, 37.1° N)	2019/7/11-2019/7/31	11-12h
Tazhong– Minfeng route	Desert Cropland Desert	8	(82.9° E, 37.5° N) (80.1° E, 37.1° N) (80.1° E, 37.4° N)	2019/7/23-2019/8/1	2-3h



	Desert		(81° E, 38.6° N)		
	Grassland		(75.2° E, 37.8° N)		
	Grassland		(76° E, 39.5° N)		
	Grassland		(82.8° E, 37.1° N)		
Ngari		50	(79.7° E, 33.4° N)	2019/7/7-2019/7/31	11-12h
Namtso	Alpine meadow	80	(91.0° E, 30.8° N)	2020/8/3-2020/8/24	9-13h
	Urban				
	Alpine meadow		(101.8° E, 36.6° N)		
	Sparse		(99.8° E, 36.7° N)		
Qinghai	grassland	8	(99.1° E, 36.8° N)	2020/7/16-2020/7/20	2-12h
	Urban		(100.1° E, 37.3° N)		
	Cropland and urban		(100.3° E, 38.2° N) (101.5° E, 37.5° N)		
	Cropland				
Yuzhong	Grassland	62	(104.1° E, 36.0° N)	2020/10/31-2020/11/19	2-6h
Yadong	Forest	141	(88.9° E, 27.4° N)	2021/6/22-2021/8/30	11-13h

105 2.2 Sampling methods

A custom-designed bioaerosol sampler was employed for field collection to ensure operational stability and methodological consistency across sites. Instruments of this type have been widely used in bioaerosol research (Maki et al., 2010; Qi et al., 2023). To construct the sampler, a 13-mm polycarbonate membrane with 0.2 µm pore size (Whatman 111106 and GTTP01300) was inserted inside a 13-mm Swinnex filter holder (Millipore SX0001300) fitted. Polycarbonate membranes offer advantages such as high chemical resistance, high thermal stability, and a low tendency to adsorb proteins or extractable substances (Ferguson et al., 2019). Their optical transparency also enables accurate microscopic detection. A micro air pump (AS ONE MAS-1, Japan) with a standard flow rate of 12 L min⁻¹ was connected to the sampler to draw atmospheric microorganisms onto the filter membrane (Fig. 2a, b).

Prior to sampling, both the filters and filter holders were sterilized. The assemblies were first rinsed with 75% ethanol, followed by ultrapure water to remove residual detergent. Subsequent processing of the filters and holders was conducted in a laminar-flow hood, where they were immersed in absolute ethanol and ultrapure water to further remove adhered organic residues. The dried filters and holders were then assembled and sterilized by autoclaving at 121 °C for 20 min, followed by ultraviolet irradiation for 30 min (Xue et al., 2024; Qi et al., 2021). The sterilized components were sealed in pre-sterilized collection tubes and sterile bags until use. During sampling, operators wore masks and sterile gloves, and the samplers were mounted at



120 a height of 1.5 m above ground level. Real-time flowmeter readings obtained immediately before the micro-pump was turned
on and immediately before it was turned off were recorded as the initial and final sampling flow rates, respectively. After
sampling, filters were labeled with the sampling location and time, stored at $-20\text{ }^{\circ}\text{C}$ during transport, and subsequently
transferred to $-80\text{ }^{\circ}\text{C}$ freezers for long-term preservation.

2.3 Fluorescence microscopy analysis

125 Bioaerosol particle concentrations were determined using DAPI staining (4,6-diamidino-2-phenylindole; D9542, Sigma),
followed by fluorescence microscopy. 4% paraformaldehyde (250 μL) was introduced to each filter holder containing the
membrane to fix the samples for 1–2 h. The filters were then rinsed with sterile ultrapure water to remove residual fixative.
Under light-protected conditions, DAPI solution (10 $\mu\text{g mL}^{-1}$, 250 μL) was introduced to stain the samples for approximately
15 min (Maki et al., 2014), followed by a final rinse with sterile water.

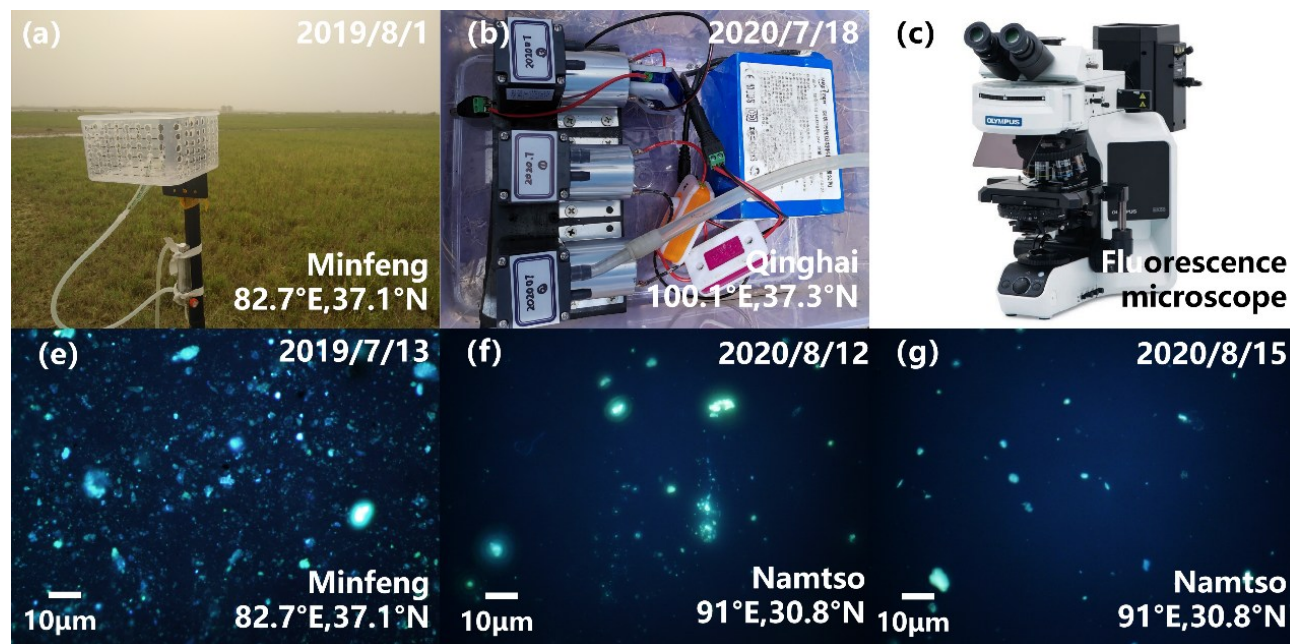
130 During slide preparation, the membrane was treated with non-fluorescent immersion oil (IMMOIL-F30CC, Olympus) for
wetting. The coverslip was then pressed firmly, and excess immersion oil was removed using a dust-free wipe. Samples were
examined using a fluorescence microscope (BX53 and DP72, Olympus) with an excitation wavelength range of 340–390 nm
A fluorescence microscope (BX53 and DP72, Olympus) providing a 340–390 nm excitation wavelength range was employed
to examine the samples. (Tang et al., 2018).

135 As shown in Fig. 2e–g, four categories of particles were distinguishable under the fluorescence microscope based on their
emitted colors: blue, yellow, white, and black. DAPI-stained microbial cells produced strong blue or blue-green fluorescence,
whereas mineral particles appeared white (Maki et al., 2013). Black particles were attributed to black carbon (Liu et al., 2023).
Yellow particles were generally interpreted as non-DNA-containing particles (Kepner and Pratt, 1994). However, other studies
have shown that water-soluble salts (Liu et al., 2023) and organic matter (Mostajir et al., 1995) can also exhibit yellow
140 fluorescence. In this study, most yellow-green particles were associated with mineral dust and were therefore considered to be
mineral particles enriched in water-soluble salts and organic material. In this study, bioaerosols were defined as particles
exhibiting cellular morphology and emitting blue-green fluorescence after DAPI staining. For each filter membrane, 20
randomly selected microscopic fields were imaged, and all particles belonging to the four categories were manually counted
using the Cell Counter plugin in ImageJ.

145 Bioaerosol number concentrations, C (particles m^{-3}) were calculated using Eq. (1):

$$C = \frac{S_1 \times N_0}{S_0 \times V}, \quad (1)$$

where S_1 is the filtration area of the filter membrane (μm^2), S_0 is the field-of-view area of the microscope (μm^2), V is the
sampled air volume (m^3), and N_0 is the average number of microbial particles observed per microscopic field of view (Maki
et al., 2019).



150

Figure 2: (a) Bioaerosols sampler used during the DuBi field sampling campaign; (b) power supply and sampling pump; (c) fluorescence microscope; (e–g) fluorescence micrographs of samples after DAPI staining.

2.4 16S rRNA gene sequencing

The 16S rRNA gene has been widely used to characterize microbial community composition and diversity (Giles et al., 2023; Nagarajan et al., 2023). The UltraClean Soil DNA Kit (MoBio, San Diego, CA) was employed to extract bacterial DNA in this study. Sequencing was performed on Illumina NovaSeq 6000 and Illumina MiSeq platforms in PE250, PE150, or PE300 modes. The bacterial 16S rRNA gene V4–V5 hypervariable region was amplified using the 515F/907R primer pair (forward: GTGCCAGCMGCCGCGGTAA; reverse: CCGTCAATTCMTTTRAGTTT) (Fang et al., 2017). Paired-end sequencing produced reads exceeding 250 bp for each sample, which were subsequently sorted according to their unique barcode sequences. Blank controls were processed alongside the samples during both DNA extraction and PCR amplification. No PCR amplicons were detected in these controls, demonstrating that the entire experimental workflow was free from detectable contamination (Qi et al., 2023; Karstens et al., 2019).

The Quantitative Insights into Microbial Ecology pipeline (QIIME2; version 2024.2) was used to assign taxonomic identities to the raw sequences (Bolyen et al., 2019). High-quality sequences were denoised and resolved into amplicon sequence variants (ASVs) at single-nucleotide resolution. Taxonomic classification was assigned using the SILVA v138 reference database (Pin et al., 2021). ASVs classified as chloroplasts, mitochondria, archaea, eukaryotes, or unassigned were removed prior to downstream ecological analyses.

165



In this study, the Shannon and Chao1 indices were used to quantify the alpha diversity of microbial communities. These indices were calculated using the vegan package in R (v4.4.4). Differences in alpha diversity among surface types were assessed using the Wilcoxon rank-sum test to evaluate statistical significance (Loos et al., 2024).

2.5 Meteorological and air quality Data

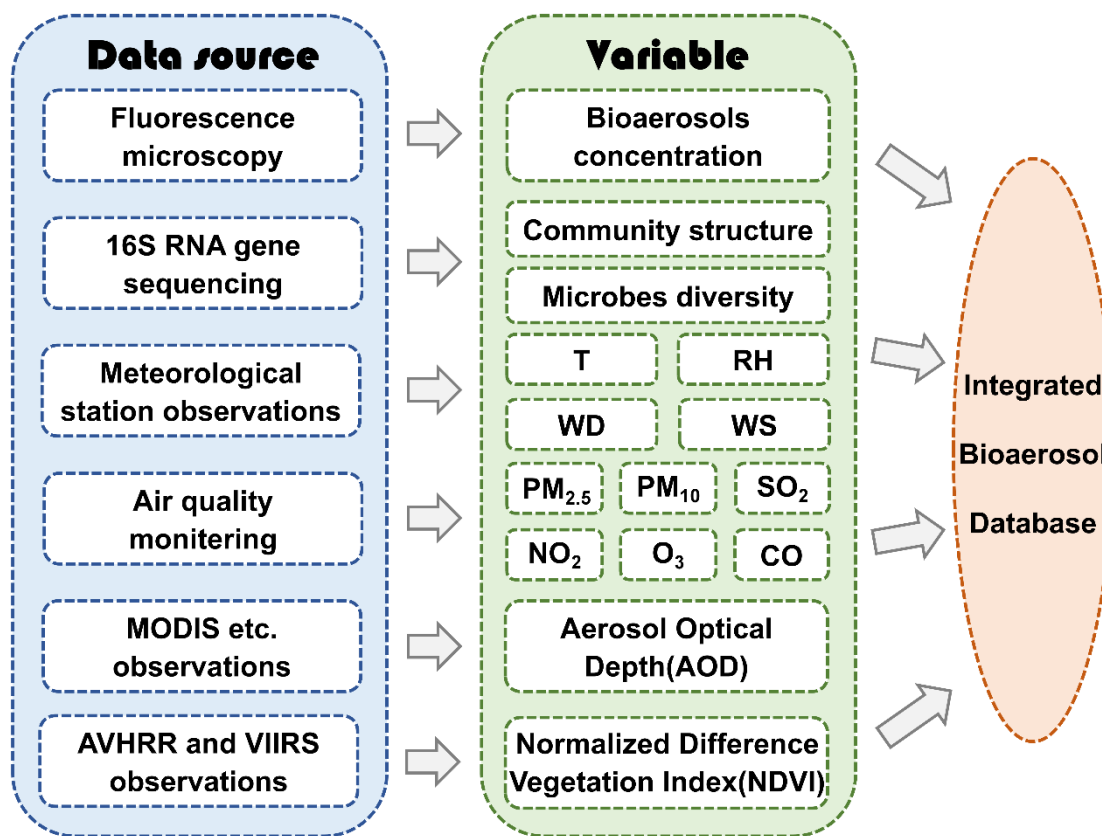


Figure 3: Schematic overview of the integrated database construction workflow and data sources.

The integrated dataset compiled in this study includes the following data products (Fig. 3):

175 Meteorological variables, such as air temperature, dew point, wind speed, wind direction, were obtained from surface meteorological observation stations. Because relative humidity (RH) is not directly reported at these stations, RH was derived using the Magnus formula based on temperature and dew-point measurements. (China stations: <https://www.ncei.noaa.gov/pub/data/noaa/isd-lite/>; stations outside China: <https://www.ncei.noaa.gov/data/global-summary-of-the-day/access/>);

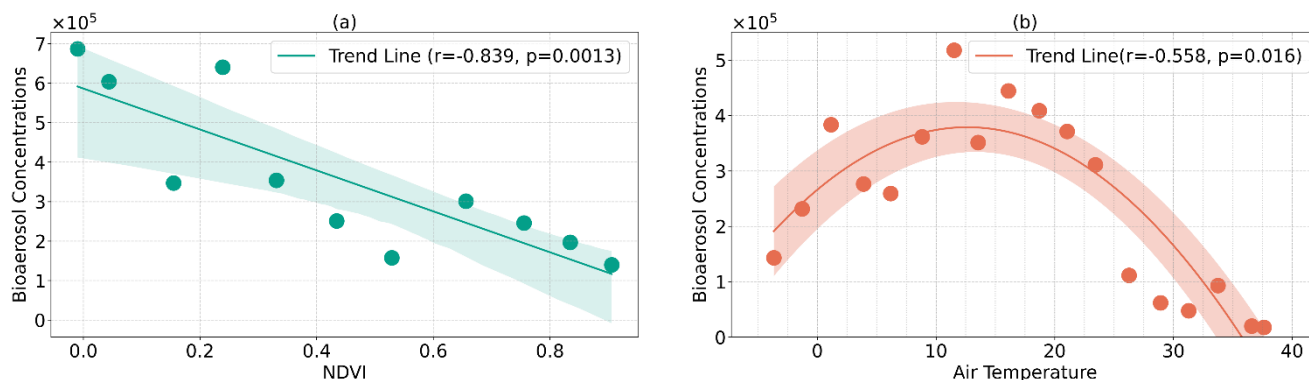


180 Air-quality data were obtained from automatic monitoring networks. For China, mass concentrations were retrieved from the
China National Urban Air Quality Real-Time Publishing Platform (<https://air.cnemc.cn:18007>). For Japan and South Korea,
data were obtained from <https://soramame.env.go.jp> and <https://www.airkorea.or.kr/>;
AOD data were obtained from two satellite-derived products. The M2IMNXGAS dataset, based on MODIS and AVHRR
retrievals, provides monthly AOD at a spatial resolution of $0.5^\circ \times 0.625^\circ$ (Gelaro et al., 2017)
185 (https://disc.gsfc.nasa.gov/datasets/M2IMNXGAS_5.12.4/summary?keywords=M2IMNXGAS_5.12.4). The MAIAC Land
AOD Level-2 product (MCD19A2, Version 6.1) provides daily aerosol optical depth (AOD) data at a spatial resolution of 1
km \times 1 km and is generated by applying the Multi-angle Implementation of Atmospheric Correction algorithm to observations
acquired from the MODIS Terra and Aqua sensors. (<https://www.earthdata.nasa.gov/data/catalog/lpcloud-mcd19a2-061>);
NDVI data were obtained from the CDR product generated from AVHRR, VIIRS, and related sensors. Data are provided on
190 a $0.05^\circ \times 0.05^\circ$ spatial grid with daily temporal coverage. (Vermote and Program, 2019) (<https://www.ncei.noaa.gov/data/land-normalized-difference-vegetation-index/access/>).

3 Results and discussion

3.1 Correlation of bioaerosol concentrations and NDVI & air temperature

We analysed the relationships between bioaerosol concentration, NDVI, and air temperature across East Asia at a large spatial
195 scale under non-special weather conditions (e.g., dust events). As shown in Fig. 4a, bioaerosol concentrations exhibit a
significant negative correlation with NDVI. In regions with low NDVI, sparse vegetation cover and dry, loose soils facilitate
the entrainment and emission of microorganisms into the atmosphere under wind forcing (Qi et al., 2023). In contrast, regions
with high NDVI are characterized by stronger vegetation-mediated particle interception, which enhances dry deposition and
consequently leads to lower atmospheric microbial concentrations (Zhai et al., 2022).
200 Figure 4b indicates that the relationship between temperature and bioaerosol concentration is non-linear. When temperatures
are below approximately 15 °C, bioaerosol concentrations show a positive correlation with temperature. However, as
temperature increases further, microbial concentrations decline markedly. A possible explanation is that, within an optimal
temperature range, warming enhances atmospheric mixing and air movement, thereby promoting the dispersal of
microorganisms into the atmosphere and resulting in higher concentrations (Cavicchioli et al., 2019). At excessively high
205 temperatures, however, conditions become unfavorable for microbial growth and reproduction, and the abundance of
microorganisms from certain sources may decrease accordingly (Zhang et al., 2022b).



210 **Figure 4: (a) Relationship between bioaerosol concentration and NDVI during the DuBi field sampling campaign. The green points represent mean bioaerosol concentrations calculated by binning NDVI into intervals of 0.1 and averaging all samples within each interval. (b) Relationship between bioaerosol concentration and air temperature. The orange points represent mean bioaerosol concentrations calculated by binning temperature into intervals of 2.5 °C and averaging all samples within each interval. The shaded areas indicate the 95 % confidence intervals.**

3.2 Diurnal variation of bioaerosol concentration

215 Figure 5 shows the temporal variations in bioaerosol concentrations in Yuzhong, China, on 6 and 15 November 2020. As illustrated, bioaerosol concentrations on both days exhibit pronounced diurnal patterns rather than random fluctuations. Concentrations are lowest in the early morning (07:00–09:00), followed by a gradual increase, reaching a peak in the afternoon (15:00–17:00), and then decreasing thereafter. This pattern suggests that bioaerosol concentrations are governed by well-defined diurnal processes.

220 The concentrations of NO_2 and CO also display clear temporal variations with similar overall trends, suggesting that these two trace gases may share common sources. However, the temporal variations of NO_2 and CO on the two sampling days are not fully consistent with those of bioaerosol concentrations. This discrepancy implies that short-term variations in bioaerosol concentrations during the sampling period were not primarily controlled by anthropogenic emissions or changes in the atmospheric boundary layer height (Li et al., 2022). Instead, they are more likely associated with surface biological emissions and atmospheric dynamical processes. These processes include daytime increases in surface temperature that enhance
225 microbial activity, intensified release from soil and vegetation surfaces, and strengthened surface turbulence that facilitates the entrainment of particles into the atmosphere (Gashi et al., 2025; Sharma et al., 2022; Zhang et al., 2022a; Kulmala et al., 2023).

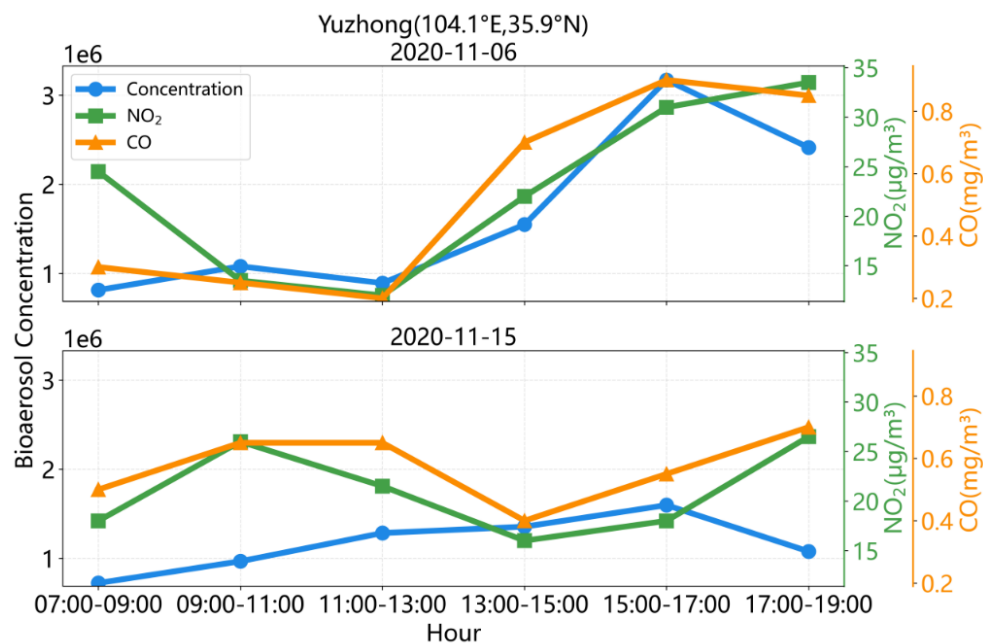


Figure 5: Temporal variations in bioaerosol concentration, NO₂, and CO in Yuzhong on 6 and 15 November 2020.

Figure 6 illustrates diurnal-scale variations in bioaerosol concentrations and related physical parameters in Yonago, Japan, from March to June 2018. As shown, bioaerosol concentrations exhibit pronounced high-frequency fluctuations on the diurnal timescale, indicating strong modulation by short-timescale processes. Within each month, concentrations consistently increase and then decrease, forming a recurrent “single-peak, within-month” pattern throughout March–June. This suggests that bioaerosols do not behave as random background noise but instead represent an aerosol component characterized by a well-defined temporal structure.

During the sampling period, a prominent concentration peak occurred in mid-April, substantially exceeding levels observed in other months and persisting for several consecutive days rather than representing a single-day anomaly. Given that no corresponding extreme peaks are observed in the other variables shown in the figure, this event is unlikely to have been driven solely by particulate matter (PM) or gaseous pollution. Instead, it more plausibly reflects a regional-scale, concentrated release from biological sources.

AOD at 550 nm reaches near-maximum values during the major bioaerosol concentration peaks and varies largely in phase with bioaerosol concentrations. The temporal variations in PM₁₀ and PM_{2.5} concentrations are broadly consistent with those of bioaerosol concentrations, with PM_{2.5} exhibiting a slight lag. This indicates that, during this event, bioaerosols and non-biological particles were influenced by shared controlling processes rather than varying independently.

In contrast, the variations in NO₂ and O₃ concentrations are substantially smaller than those of PM and bioaerosols and do not show pronounced increases or decreases concurrent with bioaerosol peaks. This indicates that the observed bioaerosol concentration variations during the sampling period were not primarily controlled by gaseous pollutant emissions.

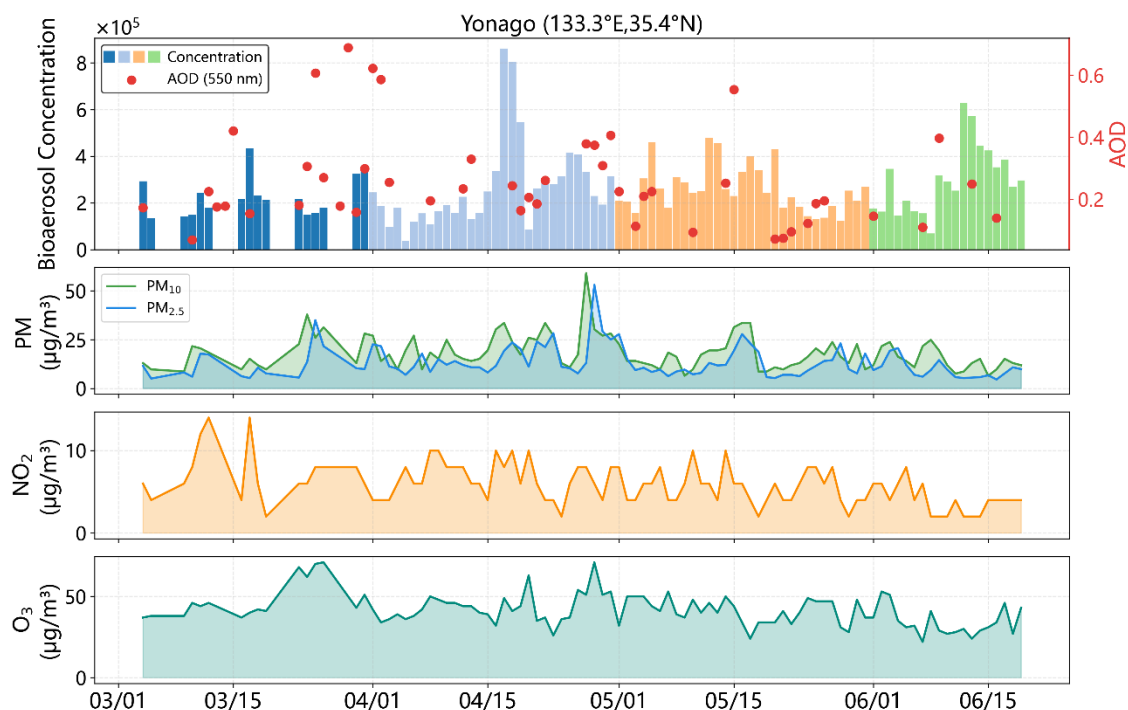


Figure 6: Daily variations in bioaerosol concentration, aerosol optical depth (AOD), PM_{2.5}, PM₁₀, NO₂, and O₃ in Yonago, Japan, during March–June 2018.

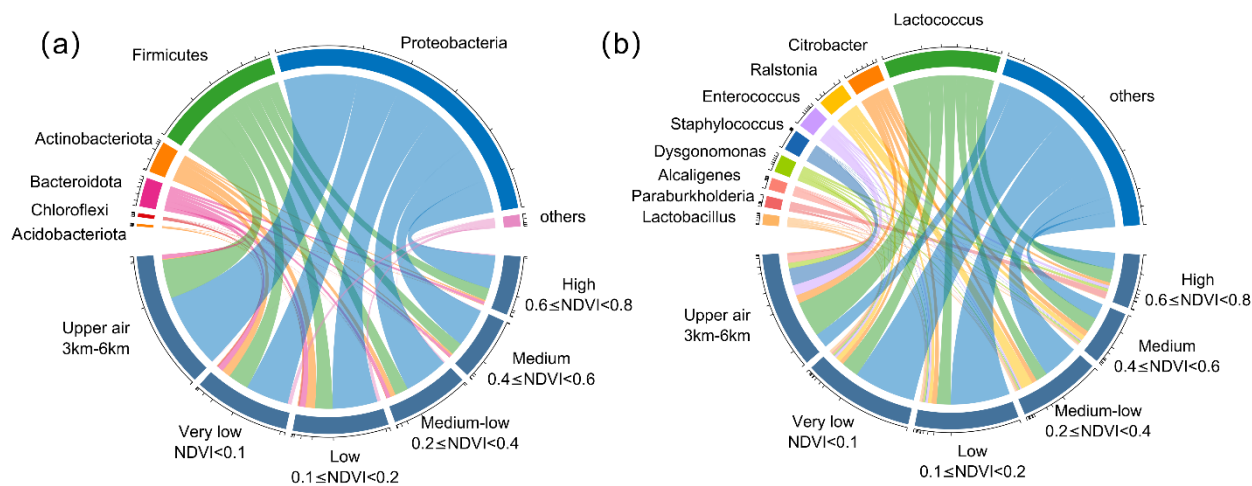
250 3.3 Bacterial community structure

To investigate the dominant taxa at different hierarchical levels across varying underlying surface types, this study selected the five taxa with the highest relative abundances for each surface type for analysis. The underlying surface was classified into six categories based on NDVI: $NDVI < 0.1$ was defined as very low vegetation cover; $0.1 \leq NDVI < 0.2$ as low vegetation cover; $0.2 \leq NDVI < 0.4$ as medium–low vegetation cover; $0.4 \leq NDVI < 0.6$ as medium vegetation cover; and $0.6 \leq NDVI \leq$
255 0.8 as high vegetation cover. In addition, because the sampling campaign included aircraft measurements, an additional category representing the upper atmosphere was included.

Figure 7a presents the bacterial community composition at the phylum level. Proteobacteria dominate the community, with a relative abundance of 60.1%, followed by Firmicutes (24.8%). Among the identified phyla, Chloroflexi are primarily associated with areas of low vegetation cover (43.0%) and very low vegetation cover (33.2%). Actinobacteria and
260 Acidobacteriota exhibit similar distribution patterns, occurring mainly in low-vegetation (33.9% and 35.3%, respectively) and very low vegetation cover regions (31.3% and 28.0%, respectively). These three phyla represent dominant bacterial groups in soils under varying vegetation conditions (Zhou and Wang, 2023). As soil and vegetation are important sources of airborne microorganisms, contributions from soil sources to atmospheric microbial populations become more pronounced under conditions of low vegetation cover (Archer et al., 2023; Xie et al., 2020).



265 Figure 7b shows the bacterial community composition at the genus level. The dominant taxon at the genus level is *Lactococcus*,
with a relative abundance of 23.4%. Among the identified genera, *Staphylococcus* (87.8%), *Alcaligenes* (67.3%), and
Enterococcus (49.6%) are predominantly distributed in the upper atmosphere. *Paraburkholderia* (61.6%) is mainly distributed
in areas with high vegetation cover. The pronounced enrichment of *Staphylococcus*, *Alcaligenes*, and *Enterococcus* in upper-
atmosphere samples may be attributed to their strong environmental tolerance and diverse source characteristics, which
270 facilitate survival during atmospheric vertical transport and under selective filtering processes in upper-atmosphere
environments (García-Solache and Rice, 2019; Onyango and Alreshidi, 2018; Machado et al., 2023; Pedrosa-Silva and
Venancio, 2023). *Paraburkholderia*, a genus typically associated with plants, receives sustained and stable biological inputs
in regions with high vegetation cover, making it more likely to accumulate in near-surface air over densely vegetated areas
(Esmael et al., 2018; Eberl and Vandamme, 2016).



275

Figure 7: (a) Distribution of dominant taxa at the phylum level across different underlying surface types; (b) distribution of dominant taxa at the genus level across different underlying surface types.

3.4 Bacterial diversity

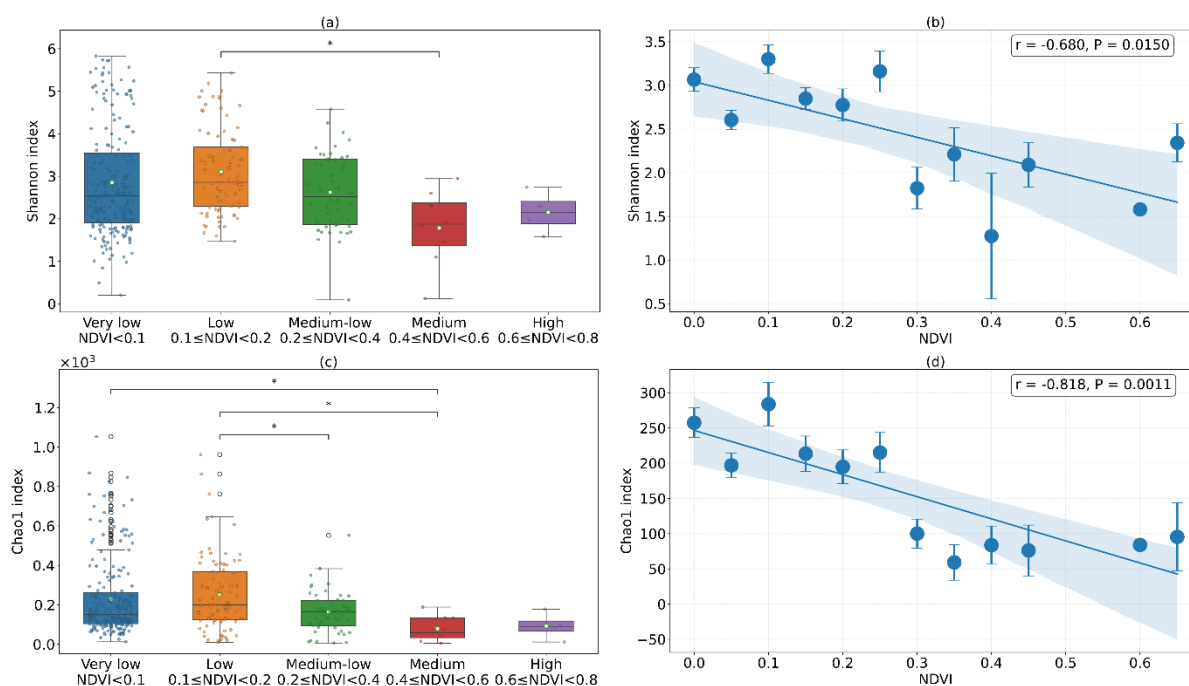
As shown in Fig. 8a and Fig. 8c, the mean values of both the Shannon and Chao1 indices across different underlying surface
280 types follow the same decreasing order: low vegetation cover > very low vegetation cover > medium–low vegetation cover >
high vegetation cover > medium vegetation cover. This pattern indicates that α diversity and species richness are highest in
areas with low vegetation cover, whereas areas with medium vegetation cover exhibit the lowest diversity. Variations in α
diversity across vegetation cover gradients reflect the combined effects of source inputs, multi-source mixing, and ecological
filtering processes (Mantoani et al., 2024; Lu et al., 2024; Gashi et al., 2025). Low vegetation cover areas integrate both soil-
285 and vegetation-derived biological sources and are typically associated with stronger surface disturbance, resulting in the
highest species richness and diversity (Nie et al., 2024; Mu et al., 2020; Archer et al., 2023). In contrast, medium vegetation
cover regions suppress soil resuspension while not yet developing the complex phyllosphere-associated microbial sources



characteristic of highly vegetated areas. Consequently, these regions experience fewer source inputs and stronger environmental filtering, leading to the lowest α diversity (Zhai et al., 2022; Robinson et al., 2021).

290 Figures 8b and 8d further show that both the Shannon index ($r = -0.68$, $P = 0.015$) and the Chao1 index ($r = -0.818$, $P = 0.0011$) are negatively correlated with NDVI, with the Chao1 index exhibiting a stronger correlation. Based on the differing sensitivities of these two indices, it can be inferred that, under low-NDVI conditions, atmospheric microbial communities are more strongly influenced by external source inputs, leading to increased species richness. However, many of the newly introduced taxa occur at low relative abundances and therefore have a limited effect on community evenness, resulting in a

295 smaller magnitude of change in the Shannon index compared to the Chao1 index.



300 **Figure 8: (a) Relationship between underlying surface types and the Shannon index; (b) relationship between NDVI and the Shannon index; (c) relationship between underlying surface types and the Chao1 index; (d) relationship between NDVI and the Chao1 index. Note: In panels (a) and (c), asterisks indicate statistically significant differences in diversity indices between sample groups based on the Wilcoxon rank-sum test, whereas the absence of asterisks indicates no significant difference. One to four asterisks denote $P < 0.05$, $P < 0.01$, $P < 0.001$, and $P < 0.0001$, respectively. In panels (b) and (d), blue dots represent mean diversity indices calculated by binning NDVI into intervals of 0.05 and averaging all samples within each bin; error bars indicate the standard error of the mean for each bin.**

Data availability

305 Interested researchers can download the integrated dataset from <https://zenodo.org/records/19605145> (Huang et al., 2026). The non-biological aerosol particle number concentration data and the bacterial community structure data at the domain, class,



order, family, and species levels during the sampling period are not currently publicly available. These data are available from the corresponding author upon reasonable request.

Conclusions

310 This study reports an integrated dataset of atmospheric bioaerosols obtained from a large-scale dust–bioaerosol field
observation campaign conducted across East Asia using a unified sampling and analytical protocol. The dataset includes
number concentrations of both biological and non-biological aerosols, bacterial community structure at multiple taxonomic
levels, together with concurrent environmental variables and air quality parameters. The database enables the systematic
analysis of correlations between regional-scale vegetation cover, temperature, and airborne microbial concentrations and
315 community structure. The results indicate that bioaerosol concentrations exhibit a significant negative correlation with NDVI.
Bioaerosol concentrations increase with air temperature below approximately 15 °C, whereas a decline is observed at higher
temperatures. Temporal-scale analysis demonstrates that the diurnal variation in bioaerosol concentration exhibits a discernible
intraday structure rather than random fluctuations. In addition, the daily evolution of bioaerosol concentrations shows a
relatively high degree of synchrony with AOD and particulate matter concentrations. Community structure and diversity
320 analyses further demonstrate pronounced ecological differentiation among regions with varying vegetation cover, with α -
diversity showing a significant negative correlation with NDVI. By integrating concentration data, community structure, and
multifactor environmental information within a unified methodological framework, this database constitutes a consistent and
comprehensive foundation for investigating land–atmosphere interface ecological processes and the spatiotemporal evolution
of regional bioaerosols, with clear substantial scientific and applied value.

325 Author contributions

JH and ZH conceived and designed the database framework, established the unified sampling and analytical protocols, and
supervised the overall project, including data validation and quality control. TM, JS and JB contributed to methodological
development, provided technical support, and assisted in data validation and manuscript revision. QD, FX, YW, YJ, XH, DL,
DW and WZ conducted field sampling and laboratory analyses and curated the dataset. WZ and QD performed the formal data
330 analysis and prepared the figures. WZ prepared the manuscript with contributions from all co-authors. All authors reviewed
and approved the final manuscript.

Competing interests

The authors declare no conflicts of interest.



Financial support

- 335 This research was financially supported by the National Key Research and Development Program of China (Grant No. 2023YFC3708202), the National Natural Science Foundation of China (Grant No. 42421001), the Gansu Science and Technology Major Program (Grant No. 24ZDWA006), and the Self-supporting Program of Guangzhou Laboratory (Grant No. GZNL2024A01004).

References

- 340 Alfaro-Perez, C., Barberá-Riera, M., de Llanos, R., and Delgado-Saborit, J. M.: Systematic review and meta-analysis of methodological approaches for characterising airborne SARS-CoV-2 RNA for environmental surveillance, *npj Climate and Atmospheric Science*, 8, 10.1038/s41612-025-01180-z, 2025.
- Araujo, D. S. A., Enquist, B. J., Frazier, A. E., Merow, C., Roehrdanz, P. R., Moulatlet, G. M., Zvoleff, A., Song, L., Maitner, B., and Nikolopoulos, E. I.: Global Future Drought Layers Based on Downscaled CMIP6 Models and Multiple Socioeconomic Pathways, *Scientific Data*, 12, 10.1038/s41597-025-04612-w, 2025.
- 345 Archer, S. D. J., Lee, K. C., Caruso, T., Alcamí, A., Araya, J. G., Cary, S. C., Cowan, D. A., Etchebehere, C., Gantsetseg, B., Gomez-Silva, B., Hartery, S., Hogg, I. D., Kansour, M. K., Lawrence, T., Lee, C. K., Lee, P. K. H., Leopold, M., Leung, M. H. Y., Maki, T., McKay, C. P., Al Mailem, D. M., Ramond, J.-B., Rastrojo, A., Šantl-Temkiv, T., Sun, H. J., Tong, X., Vandenbrink, B., Warren-Rhodes, K. A., and Pointing, S. B.: Contribution of soil bacteria to the atmosphere across biomes, *Science of The Total Environment*, 871, 10.1016/j.scitotenv.2023.162137, 2023.
- 350 Balvočiūtė, M. and Huson, D. H.: SILVA, RDP, Greengenes, NCBI and OTT — how do these taxonomies compare?, *BMC Genomics*, 18, 10.1186/s12864-017-3501-4, 2017.
- Boifot, K. O., Skogan, G., and Dybwad, M.: Sampling efficiency and nucleic acid stability during long-term sampling with different bioaerosol samplers, *Environ Monit Assess*, 196, 577, 10.1007/s10661-024-12735-7, 2024.
- 355 Bolyen, E., Rideout, J. R., Dillon, M. R., Bokulich, N. A., Abnet, C. C., Al-Ghalith, G. A., Alexander, H., Alm, E. J., Arumugam, M., Asnicar, F., Bai, Y., Bisanz, J. E., Bittinger, K., Brejnrod, A., Brislawn, C. J., Brown, C. T., Callahan, B. J., Caraballo-Rodríguez, A. M., Chase, J., Cope, E. K., Da Silva, R., Diener, C., Dorrestein, P. C., Douglas, G. M., Durall, D. M., Duvall, C., Edwardson, C. F., Ernst, M., Estaki, M., Fouquier, J., Gauglitz, J. M., Gibbons, S. M., Gibson, D. L., Gonzalez, A., Gorlick, K., Guo, J., Hillmann, B., Holmes, S., Holste, H., Huttenhower, C., Huttley, G. A., Janssen, S., Jarmusch, A. K., Jiang, L., Kaehler, B. D., Kang, K. B., Keefe, C. R., Keim, P., Kelley, S. T., Knights, D., Koester, I., Kosciulek, T., Kreps, J., Langille, M. G. I., Lee, J., Ley, R., Liu, Y.-X., Loftfield, E., Lozupone, C., Maher, M., Marotz, C., Martin, B. D., McDonald, D., McIver, L. J., Melnik, A. V., Metcalf, J. L., Morgan, S. C., Morton, J. T., Naimey, A. T., Navas-Molina, J. A., Nothias, L. F., Orchanian, S. B., Pearson, T., Peoples, S. L., Petras, D., Preuss, M. L., Pruesse, E., Rasmussen, L. B., Rivers, A., Robeson, M. S., Rosenthal, P., Segata, N., Shaffer, M., Shiffer, A., Sinha, R., Song, S. J., Spear, J. R., Swafford, A. D., Thompson, L.
- 360 R., Torres, P. J., Trinh, P., Tripathi, A., Turnbaugh, P. J., Ul-Hasan, S., van der Hooft, J. J. J., Vargas, F., Vázquez-Baeza, Y.,



- Vogtmann, E., von Hippel, M., Walters, W., Wan, Y., Wang, M., Warren, J., Weber, K. C., Williamson, C. H. D., Willis, A. D., Xu, Z. Z., Zaneveld, J. R., Zhang, Y., Zhu, Q., Knight, R., and Caporaso, J. G.: Reproducible, interactive, scalable and extensible microbiome data science using QIIME 2, *Nature Biotechnology*, 37, 852-857, 10.1038/s41587-019-0209-9, 2019.
- 370 Bulski, K.: Bioaerosols at plants processing materials of plant origin—a review, *Environmental Science and Pollution Research*, 27, 27507-27514, 10.1007/s11356-020-09121-4, 2020.
- Cavicchioli, R., Ripple, W. J., Timmis, K. N., Azam, F., Bakken, L. R., Baylis, M., Behrenfeld, M. J., Boetius, A., Boyd, P. W., Classen, A. T., Crowther, T. W., Danovaro, R., Foreman, C. M., Huisman, J., Hutchins, D. A., Jansson, J. K., Karl, D. M., Koskella, B., Mark Welch, D. B., Martiny, J. B. H., Moran, M. A., Orphan, V. J., Reay, D. S., Remais, J. V., Rich, V. I., Singh, B. K., Stein, L. Y., Stewart, F. J., Sullivan, M. B., van Oppen, M. J. H., Weaver, S. C., Webb, E. A., and Webster, N. S.:
375 Scientists' warning to humanity: microorganisms and climate change, *Nature Reviews Microbiology*, 17, 569-586, 10.1038/s41579-019-0222-5, 2019.
- Clasen, L. A., Detheridge, A. P., Scullion, J., and Griffith, G. W.: Soil stabilisation for DNA metabarcoding of plants and fungi. Implications for sampling at remote locations or via third-parties, *Metabarcoding and Metagenomics*, 4, <https://doi.org/10.3897/mbmg.4.58365>, 2020.
- 380 Després, V. R., Huffman, J. A., Burrows, S. M., Hoose, C., Safatov, A. S., Buryak, G., Fröhlich-Nowoisky, J., Elbert, W., Andreae, M. O., Pöschl, U., and Jaenicke, R.: Primary biological aerosol particles in the atmosphere: a review, *Tellus B: Chemical and Physical Meteorology*, 64, 10.3402/tellusb.v64i0.15598, 2012.
- Du, P., Du, R., Ren, W., Lu, Z., and Fu, P.: Seasonal variation characteristic of inhalable microbial communities in PM_{2.5} in Beijing city, China, *Science of The Total Environment*, 610-611, 308-315, 10.1016/j.scitotenv.2017.07.097, 2018.
- 385 Eberl, L. and Vandamme, P.: Members of the genus *Burkholderia*: good and bad guys, *F1000Research*, 5, 10.12688/f1000research.8221.1, 2016.
- Eriksen, E., Afanou, A. K., Madsen, A. M., Straumfors, A., and Graff, P.: An assessment of occupational exposure to bioaerosols in automated versus manual waste sorting plants, *Environmental Research*, 218, 10.1016/j.envres.2022.115040, 2023.
- 390 Esmacel, Q., Miotto, L., Rondeau, M., Leclere, V., Clement, C., Jacquard, C., Sanchez, L., and Barka, E. A.: Paraburkholderia phytotfirmans PsJN-Plants Interaction: From Perception to the Induced Mechanisms, *Front Microbiol*, 9, 2093, 10.3389/fmicb.2018.02093, 2018.
- Estillore, A. D., Trueblood, J. V., and Grassian, V. H.: Atmospheric chemistry of bioaerosols: heterogeneous and multiphase reactions with atmospheric oxidants and other trace gases, *Chemical Science*, 7, 6604-6616, 10.1039/c6sc02353c, 2016.
- 395 Fang, H., Chen, Y., Huang, L., and He, G.: Analysis of biofilm bacterial communities under different shear stresses using size-fractionated sediment, *Scientific Reports*, 7, 1299, 10.1038/s41598-017-01446-4, 2017.
- Ferguson, R. M. W., Garcia-Alcega, S., Coulon, F., Dumbrell, A. J., Whitby, C., and Colbeck, I.: Bioaerosol biomonitoring: Sampling optimization for molecular microbial ecology, *Molecular Ecology Resources*, 19, 672-690, 10.1111/1755-0998.13002, 2019.



- 400 Fröhlich-Nowoisky, J., Kampf, C. J., Weber, B., Huffman, J. A., Pöhlker, C., Andreae, M. O., Lang-Yona, N., Burrows, S. M.,
Gunthe, S. S., Elbert, W., Su, H., Hoor, P., Thines, E., Hoffmann, T., Després, V. R., and Pöschl, U.: Bioaerosols in the Earth
system: Climate, health, and ecosystem interactions, *Atmospheric Research*, 182, 346-376, 10.1016/j.atmosres.2016.07.018,
2016.
- García-Solache, M. and Rice, L. B.: The Enterococcus: a Model of Adaptability to Its Environment, *Clinical Microbiology*
405 *Reviews*, 32, 10.1128/cmr.00058-18, 2019.
- Gashi, N., Szóke, Z., Fauszt, P., Dávid, P., Mikolás, M., Gál, F., Stündl, L., Remenyik, J., and Paholcsek, M.: Bioaerosols in
Agriculture: A Comprehensive Approach for Sustainable Crop Health and Environmental Balance, *Agronomy*, 15,
10.3390/agronomy15051003, 2025.
- Gelaro, R., McCarty, W., Suárez, M. J., Todling, R., Molod, A., Takacs, L., Randles, C. A., Darmenov, A., Bosilovich, M. G.,
410 Reichle, R., Wargan, K., Coy, L., Cullather, R., Draper, C., Akella, S., Buchard, V., Conaty, A., da Silva, A. M., Gu, W., Kim,
G.-K., Koster, R., Lucchesi, R., Merkova, D., Nielsen, J. E., Partyka, G., Pawson, S., Putman, W., Rienecker, M., Schubert, S.
D., Sienkiewicz, M., and Zhao, B.: The Modern-Era Retrospective Analysis for Research and Applications, Version 2
(MERRA-2), *Journal of Climate*, 30, 5419-5454, 10.1175/jcli-d-16-0758.1, 2017.
- Giles, M. E., Caul, S., King, D., Mitchell, S., Sim, A., Neilson, R., and Paterson, E.: Grass variety selection of microbial
415 community composition is associated with differences in soil CO₂ emissions, *Applied Soil Ecology*, 190,
10.1016/j.apsoil.2023.104968, 2023.
- Guo, J., Lv, M., Liu, Z., Qin, T., Qiu, H., Zhang, L., Lu, J., Hu, L., Yang, W., and Zhou, D.: Comprehensive performance
evaluation of six bioaerosol samplers based on an aerosol wind tunnel, *Environ Int*, 183, 108402,
10.1016/j.envint.2023.108402, 2024.
- 420 Hofmann, W.: Modelling inhaled particle deposition in the human lung—A review, *Journal of Aerosol Science*, 42, 693-724,
10.1016/j.jaerosci.2011.05.007, 2011.
- Hoose, C. and Möhler, O.: Heterogeneous ice nucleation on atmospheric aerosols: a review of results from laboratory
experiments, *Atmospheric Chemistry and Physics*, 12, 9817-9854, 10.5194/acp-12-9817-2012, 2012.
- Huang, Z., Wang, Y., Zhou, T., Ji, Y., Bi, J., Shi, J., Wen, H., and Huang, J.: Raman-Polarization-Fluorescence Spectroscopic
425 Lidar for Real-Time Detection of Humic-like Substance Profiles, *Environmental Science & Technology*, 59, 7235-7245,
10.1021/acs.est.5c00028, 2025.
- Huang, Z., Yu, X., Liu, Q., Maki, T., Alam, K., Wang, Y., Xue, F., Tang, S., Du, P., Dong, Q., Wang, D., and Huang, J.:
Bioaerosols in the atmosphere: A comprehensive review on detection methods, concentration and influencing factors, *Science*
of The Total Environment, 912, 10.1016/j.scitotenv.2023.168818, 2024a.
- 430 Huang, Z., Dong, Q., Xue, F., Qi, J., Yu, X., Maki, T., Du, P., Gu, Q., Tang, S., Shi, J., Bi, J., Zhou, T., and Huang, J.: Large-
Scale Dust–Bioaerosol Field Observations in East Asia, *Bulletin of the American Meteorological Society*, 105, E501-E517,
10.1175/bams-d-23-0108.1, 2024b.



- Huang, Z., Zhang, W., Dong, Q., Maki, T., Wang, Y., Ji, Y., Xue, F., Huo, X., Lu, D., Wang, D., Shi, J., Bi, J., and Huang, J.: Integrated dataset of atmospheric bioaerosols over east Asia [dataset], <https://doi.org/10.5281/zenodo.19605145>, 2026.
- 435 Jabeen, R., Kizhisseri, M. I., Mayanaik, S. N., and Mohamed, M. M.: Bioaerosol assessment in indoor and outdoor environments: a case study from India, *Scientific Reports*, 13, 10.1038/s41598-023-44315-z, 2023.
- Jeong, S. Y. and Kim, T. G.: Comparison of five membrane filters to collect bioaerosols for airborne microbiome analysis, *J Appl Microbiol*, 131, 780-790, 10.1111/jam.14972, 2021.
- Jiang, X., Wang, C., Guo, J., Hou, J., Guo, X., Zhang, H., Tan, J., Li, M., Li, X., and Zhu, H.: Global Meta-analysis of Airborne
440 Bacterial Communities and Associations with Anthropogenic Activities, *Environ Sci Technol*, 56, 9891-9902, 10.1021/acs.est.1c07923, 2022.
- Jin, J., Pang, M., Segers, A., Han, W., Fang, L., Li, B., Feng, H., Lin, H. X., and Liao, H.: Inverse modeling of the 2021 spring super dust storms in East Asia, *Atmospheric Chemistry and Physics*, 22, 6393-6410, 10.5194/acp-22-6393-2022, 2022.
- Karstens, L., Asquith, M., Davin, S., Fair, D., Gregory, W. T., Wolfe, A. J., Braun, J., and McWeeney, S.: Controlling for
445 Contaminants in Low-Biomass 16S rRNA Gene Sequencing Experiments, *mSystems*, 4, 10.1128/mSystems.00290-19, 2019.
- Kepner, R. L. and Pratt, J. R.: Use of fluorochromes for direct enumeration of total bacteria in environmental samples: past and present, *Microbiological Reviews*, 58, 603-615, 10.1128/mr.58.4.603-615.1994, 1994.
- Kulmala, M., Kokkonen, T., Ezhova, E., Baklanov, A., Mahura, A., Mammarella, I., Bäck, J., Lappalainen, H. K., Tyuryakov, S., Kerminen, V.-M., Zilitinkevich, S., and Petäjä, T.: Aerosols, Clusters, Greenhouse Gases, Trace Gases and Boundary-
450 Layer Dynamics: on Feedbacks and Interactions, *Boundary-Layer Meteorology*, 186, 475-503, 10.1007/s10546-022-00769-8, 2023.
- Larsen, P., Birtel, J., Walser, J.-C., Pichon, S., Bürgmann, H., and Matthews, B.: Estimating Bacterial Diversity for Ecological Studies: Methods, Metrics, and Assumptions, *Plos One*, 10, 10.1371/journal.pone.0125356, 2015.
- Li, J., Zuraimi, S., Schiavon, S., Wan, M. P., Xiong, J., and Tham, K. W.: Diurnal trends of indoor and outdoor fluorescent
455 biological aerosol particles in a tropical urban area, *Sci Total Environ*, 848, 157811, 10.1016/j.scitotenv.2022.157811, 2022.
- Lin, L. and Ju, F.: Evaluation of different 16S rRNA gene hypervariable regions and reference databases for profiling engineered microbiota structure and functional guilds in a swine wastewater treatment plant, *Interface Focus*, 13, 20230012, 10.1098/rsfs.2023.0012, 2023.
- Liu, T., Zhang, J., Cao, J., Zheng, H., Zhan, C., Liu, H., Zhang, L., Xiao, K., Liu, S., Xiang, D., and Zhang, D.: Identification
460 of coexistence of biological and non-biological aerosol particles with DAPI (4',6-diamidino-2-phenylindole) stain, *Particuology*, 72, 49-57, 10.1016/j.partic.2022.02.009, 2023.
- Loos, D., Filho, A. P. d. C., Dutilh, B. E., Barber, A. E., and Panagiotou, G.: A global survey of host, aquatic, and soil microbiomes reveals shared abundance and genomic features between bacterial and fungal generalists, *Cell Reports*, 43, 10.1016/j.celrep.2024.114046, 2024.



- 465 Lu, C., Xiao, Z., Li, H., Han, R., Sun, A., Xiang, Q., Zhu, Z., Li, G., Yang, X., Zhu, Y.-G., and Chen, Q.-L.: Aboveground plants determine the exchange of pathogens within air-phylosphere-soil continuum in urban greenspaces, *Journal of Hazardous Materials*, 465, 10.1016/j.jhazmat.2023.133149, 2024.
- Machado, R. A. R., Loulou, A., Bhat, A. H., Mastore, M., Terrettaz, C., Brivio, M. F., and Kallel, S.: *Acinetobacter nematophilus* sp. nov., *Alcaligenes nematophilus* sp. nov., *Enterobacter nematophilus* sp. nov., and *Kaistia nematophila* sp. nov., Isolated from Soil-Borne Nematodes and Proposal for the Elevation of *Alcaligenes faecalis* subsp. *faecalis*, *Alcaligenes faecalis* subsp. *parafaecalis*, and *Alcaligenes faecalis* subsp. *phenolicus* to the Species Level, *Taxonomy*, 3, 148-168, 10.3390/taxonomy3010012, 2023.
- Mainelis, G.: Bioaerosol sampling: Classical approaches, advances, and perspectives, *Aerosol Science and Technology*, 54, 496-519, 10.1080/02786826.2019.1671950, 2019.
- 475 Maki, T., Hara, K., Yamada, M., Kobayashi, F., Hasegawa, H., and Iwasaka, Y.: Epifluorescent Microscopic Observation of Aerosol, *Eurozoru Kenkyu*, 28, 201-207, 10.11203/jar.28.201, 2013.
- Maki, T., Puspitasari, F., Hara, K., Yamada, M., Kobayashi, F., Hasegawa, H., and Iwasaka, Y.: Variations in the structure of airborne bacterial communities in a downwind area during an Asian dust (Kosa) event, *Science of The Total Environment*, 488-489, 75-84, 10.1016/j.scitotenv.2014.04.044, 2014.
- 480 Maki, T., Susuki, S., Kobayashi, F., Kakikawa, M., Tobo, Y., Yamada, M., Higashi, T., Matsuki, A., Hong, C., Hasegawa, H., and Iwasaka, Y.: Phylogenetic analysis of atmospheric halotolerant bacterial communities at high altitude in an Asian dust (KOSA) arrival region, Suzu City, *Science of The Total Environment*, 408, 4556-4562, 10.1016/j.scitotenv.2010.04.002, 2010.
- Maki, T., Lee, K. C., Kawai, K., Onishi, K., Hong, C. S., Kurosaki, Y., Shinoda, M., Kai, K., Iwasaka, Y., Archer, S. D. J., Lacap-Bugler, D. C., Hasegawa, H., and Pointing, S. B.: Aeolian Dispersal of Bacteria Associated With Desert Dust and Anthropogenic Particles Over Continental and Oceanic Surfaces, *Journal of Geophysical Research: Atmospheres*, 124, 5579-5588, 10.1029/2018jd029597, 2019.
- Mantoani, M. C., Guerra, L. C. C., Andrade, M. F., Dias, M. A. F. S., Dias, P. L. S., Rodrigues, F., Silva, D. M. C., Filho, V. B. D., Rudke, A. P., Martins, J. A., Martins, L. D., Torezan, J. M. D., Brancalion, P. H. S., Guillemot, J., Campoe, O. C., Phillips, V., Carotenuto, F., Šantl-Temkiv, T., Morris, C. E., and Gonçalves, F. L. T.: Land-use patterns and fungal bioaerosols in the Brazilian Atlantic Forest biome, *Discover Environment*, 2, 10.1007/s44274-024-00049-x, 2024.
- 490 Mbareche, H., Veillette, M., Bilodeau, G. J., Duchaine, C., and Schaffner, D. W.: Bioaerosol Sampler Choice Should Consider Efficiency and Ability of Samplers To Cover Microbial Diversity, *Applied and Environmental Microbiology*, 84, 10.1128/aem.01589-18, 2018.
- Meinander, O., Dagsson-Waldhauserova, P., Amosov, P., Aseyeva, E., Atkins, C., Baklanov, A., Baldo, C., Barr, S. L., Barzycka, B., Benning, L. G., Cvetkovic, B., Enchilik, P., Frolov, D., Gassó, S., Kandler, K., Kasimov, N., Kavan, J., King, J., Koroleva, T., Krupskaya, V., Kulmala, M., Kusiak, M., Lappalainen, H. K., Laska, M., Lasne, J., Lewandowski, M., Luks, B., McQuaid, J. B., Moroni, B., Murray, B., Möhler, O., Nawrot, A., Nickovic, S., O'Neill, N. T., Pejanovic, G., Popovicheva, O., Ranjbar, K., Romanias, M., Samonova, O., Sanchez-Marroquin, A., Schepanski, K., Semenov, I., Sharapova, A., Shevnina,



- E., Shi, Z., Sofiev, M., Thevenet, F., Thorsteinsson, T., Timofeev, M., Umo, N. S., Uppstu, A., Urupina, D., Varga, G., Werner,
500 T., Arnalds, O., and Vukovic Vimic, A.: Newly identified climatically and environmentally significant high-latitude dust
sources, *Atmospheric Chemistry and Physics*, 22, 11889-11930, 10.5194/acp-22-11889-2022, 2022.
- Mescioglu, E., Paytan, A., Mitchell, B. W., and Griffin, D. W.: Efficiency of bioaerosol samplers: a comparison study,
Aerobiologia, 37, 447-459, 10.1007/s10453-020-09686-0, 2021.
- Morris, C. E., Conen, F., Alex Huffman, J., Phillips, V., Pöschl, U., and Sands, D. C.: Bioprecipitation: a feedback cycle
505 linking Earth history, ecosystem dynamics and land use through biological ice nucleators in the atmosphere, *Global Change
Biology*, 20, 341-351, 10.1111/gcb.12447, 2013.
- Mostajir, B., Dolan, J. R., and Rassoulzadegan, F.: A simple method for the quantification of a class of labile marine pico- and
nano-sized detritus: DAPI Yellow Particles (DYP), *Aquatic Microbial Ecology*, 9, 259-266, 10.3354/ame009259, 1995.
- Mu, F., Li, Y., Lu, R., Qi, Y., Xie, W., and Bai, W.: Source identification of airborne bacteria in the mountainous area and the
510 urban areas, *Atmospheric Research*, 231, 10.1016/j.atmosres.2019.104676, 2020.
- Nagarajan, V., Tsai, H.-C., Chen, J.-S., Koner, S., Kumar, R. S., Chao, H.-C., and Hsu, B.-M.: Systematic assessment of
mineral distribution and diversity of microbial communities and its interactions in the Taiwan subduction zone of mud
volcanoes, *Environmental Research*, 216, 10.1016/j.envres.2022.114536, 2023.
- Nie, C., Qiu, Y., Pei, T., and Qin, Y.: Specific Sources Exert Influence on the Community Structures of Bioaerosols,
515 *Aerobiology*, 2, 72-84, 10.3390/aerobiology2040006, 2024.
- Onyango, L. A. and Alreshidi, M. M.: Adaptive Metabolism in Staphylococci: Survival and Persistence in Environmental and
Clinical Settings, *Journal of Pathogens*, 2018, 1-11, 10.1155/2018/1092632, 2018.
- Pedrosa-Silva, F. and Venancio, T. M.: Comparative Genomics Reveals Novel Species and Insights into the Biotechnological
Potential, Virulence, and Resistance of *Alcaligenes*, *Genes*, 14, 10.3390/genes14091783, 2023.
- 520 Péguilhan, R., Rossi, F., Joly, M., Nasr, E., Batut, B., Enault, F., Ervens, B., and Amato, P.: Clouds influence the functioning
of airborne microorganisms, *Biogeosciences*, 22, 1257-1275, 10.5194/bg-22-1257-2025, 2025.
- Petersson Sjögren, M., Alsved, M., Šantl-Temkiv, T., Bjerring Kristensen, T., and Löndahl, J.: Measurement report:
Atmospheric fluorescent bioaerosol concentrations measured during 18 months in a coniferous forest in the south of Sweden,
Atmospheric Chemistry and Physics, 23, 4977-4992, 10.5194/acp-23-4977-2023, 2023.
- 525 Pin, L., Eiler, A., Fazi, S., and Friberg, N.: Two different approaches of microbial community structure characterization in
riverine epilithic biofilms under multiple stressors conditions: Developing molecular indicators, *Molecular Ecology Resources*,
21, 1200-1215, 10.1111/1755-0998.13341, 2021.
- Pogner, C. E., Antunes, C., Apangu, G. P., Bruffaerts, N., Celenk, S., Cristofori, A., González Roldán, N., Grinn-Gofroń, A.,
Lara, B., Lika, M., Magyar, D., Martinez-Bracero, M., Muggia, L., Muysshondt, B., O'Connor, D., Pallavicini, A., Marchã
530 Penha, M. A., Pérez-Badia, R., Ribeiro, H., Rodrigues Costa, A., Tischner, Z., Xhetani, M., and Ambelas Skjøth, C.: Airborne
DNA: State of the art – Established methods and missing pieces in the molecular genetic detection of airborne microorganisms,
viruses and plant particles, *Science of The Total Environment*, 957, 10.1016/j.scitotenv.2024.177439, 2024.



- Qi, H., Gao, X., Lei, J., Meng, X., and Hu, Z.: Transforming desertification patterns in Asia: Evaluating trends, drivers, and climate change impacts from 1990 to 2022, *Ecological Indicators*, 161, 10.1016/j.ecolind.2024.111948, 2024.
- 535 Qi, J., Huang, Z., Maki, T., Kang, S., Guo, J., Liu, K., and Liu, Y.: Airborne bacterial communities over the Tibetan and Mongolian Plateaus: variations and their possible sources, *Atmospheric Research*, 247, 10.1016/j.atmosres.2020.105215, 2021.
- Qi, J., Huang, Z., Xue, F., Gao, Z., Maki, T., Zhang, Z., Liu, K., Ji, M., and Liu, Y.: Aridification alters the diversity of airborne bacteria in drylands of China, *Atmospheric Environment*, 315, 10.1016/j.atmosenv.2023.120135, 2023.
- Ramakodi, M. P.: Influence of 16S rRNA reference databases in amplicon-based environmental microbiome research, 540 *Biotechnol Lett*, 44, 523-533, 10.1007/s10529-022-03233-2, 2022.
- Robinson, J. M., Cando-Dumancela, C., Antwis, R. E., Cameron, R., Liddicoat, C., Poudel, R., Weinstein, P., and Breed, M. F.: Exposure to airborne bacteria depends upon vertical stratification and vegetation complexity, *Scientific Reports*, 11, 10.1038/s41598-021-89065-y, 2021.
- Safatov, A. S., Andreeva, I. S., Buryak, G. A., Olkin, S. E., Reznikova, I. K., Belan, B. D., Panchenko, M. V., and Simonenkov, 545 D. V.: Long-Term Studies of Biological Components of Atmospheric Aerosol: Trends and Variability, *Atmosphere*, 13, 10.3390/atmos13050651, 2022.
- Sajjad, B., Hussain, S., Rasool, K., Hassan, M., and Almomani, F.: Comprehensive insights into advances in ambient bioaerosols sampling, analysis and factors influencing bioaerosols composition, *Environmental Pollution*, 336, 10.1016/j.envpol.2023.122473, 2023.
- 550 Samake, A., Uzu, G., Martins, J. M. F., Calas, A., Vince, E., Parat, S., and Jaffrezo, J. L.: The unexpected role of bioaerosols in the Oxidative Potential of PM, *Scientific Reports*, 7, 10.1038/s41598-017-11178-0, 2017.
- Šantl-Temkiv, T., Sikoparija, B., Maki, T., Carotenuto, F., Amato, P., Yao, M., Morris, C. E., Schnell, R., Jaenicke, R., Pöhlker, C., DeMott, P. J., Hill, T. C. J., and Huffman, J. A.: Bioaerosol field measurements: Challenges and perspectives in outdoor studies, *Aerosol Science and Technology*, 54, 520-546, 10.1080/02786826.2019.1676395, 2019.
- 555 Shammi, M., Rahman, M. M., and Tareq, S. M.: Distribution of Bioaerosols in Association With Particulate Matter: A Review on Emerging Public Health Threat in Asian Megacities, *Frontiers in Environmental Science*, 9, 10.3389/fenvs.2021.698215, 2021.
- Sharma, B., Singh, B. N., Dwivedi, P., and Rajawat, M. V. S.: Interference of Climate Change on Plant-Microbe Interaction: Present and Future Prospects, *Frontiers in Agronomy*, 3, 10.3389/fagro.2021.725804, 2022.
- 560 Tang, K., Huang, Z., Huang, J., Maki, T., Zhang, S., Shimizu, A., Ma, X., Shi, J., Bi, J., Zhou, T., Wang, G., and Zhang, L.: Characterization of atmospheric bioaerosols along the transport pathway of Asian dust during the Dust-Bioaerosol 2016 Campaign, *Atmospheric Chemistry and Physics*, 18, 7131-7148, 10.5194/acp-18-7131-2018, 2018.
- Van Leuken, J. P. G., Swart, A. N., Havelaar, A. H., Van Pul, A., Van der Hoek, W., and Heederik, D.: Atmospheric dispersion modelling of bioaerosols that are pathogenic to humans and livestock – A review to inform risk assessment studies, *Microbial* 565 *Risk Analysis*, 1, 19-39, 10.1016/j.mran.2015.07.002, 2016.



- Vermote, E. and Program, N. C.: NOAA Climate Data Record (CDR) of AVHRR Normalized Difference Vegetation Index (NDVI), Version 5 (Temporal subset: March 2011–August 2021), NOAA National Centers for Environmental Information [dataset], 10.7289/V5ZG6QH9, 2019.
- Xie, W., Li, Y., Bai, W., Hou, J., Ma, T., Zeng, X., Zhang, L., and An, T.: The source and transport of bioaerosols in the air: A review, *Frontiers of Environmental Science & Engineering*, 15, 10.1007/s11783-020-1336-8, 2020.
- Xu, F., Bento, V. A., Qu, Y., and Wang, Q.: Projections of Global Drought and Their Climate Drivers Using CMIP6 Global Climate Models, *Water*, 15, 10.3390/w15122272, 2023.
- Xue, F., Huang, Z., Huo, X., Dong, Q., Li, Z., and Gu, Q.: The Diversity of Airborne Bacteria Over the Tibet Plateau Decreased by Taklimakan Dust, *Geophysical Research Letters*, 52, 10.1029/2024gl111830, 2024.
- 575 Yu, T., Xiaole, P., Yujie, J., Yuting, Z., Weijie, Y., Hang, L., Shandong, L., and Zifa, W.: East Asia dust storms in spring 2021: Transport mechanisms and impacts on China, *Atmospheric Research*, 290, 10.1016/j.atmosres.2023.106773, 2023.
- Zawadowicz, M. A., Froyd, K. D., Perring, A. E., Murphy, D. M., Spracklen, D. V., Heald, C. L., Buseck, P. R., and Cziczo, D. J.: Model-measurement consistency and limits of bioaerosol abundance over the continental United States, *Atmospheric Chemistry and Physics*, 19, 13859-13870, 10.5194/acp-19-13859-2019, 2019.
- 580 Zhai, H., Yao, J., Wang, G., and Tang, X.: Study of the Effect of Vegetation on Reducing Atmospheric Pollution Particles, *Remote Sensing*, 14, 10.3390/rs14051255, 2022.
- Zhang, J., Li, G., Shi, L., Huang, N., and Shao, Y.: Impact of turbulence on aeolian particle entrainment: results from wind-tunnel experiments, *Atmospheric Chemistry and Physics*, 22, 9525-9535, 10.5194/acp-22-9525-2022, 2022a.
- Zhang, L., Liu, T., Zhang, J., Zhu, B., Xiang, D., Zhao, X., and Liu, X.: Bioaerosol Seasonal Variation and Contribution to Airborne Particulate Matter in Huangshi City of Central China, *Atmosphere*, 13, 10.3390/atmos13060909, 2022b.
- 585 Zhou, T., Zhou, X., Yang, Z., Córdoba-Jabonero, C., Wang, Y., Huang, Z., Da, P., Luo, Q., Zhang, Z., Shi, J., Bi, J., and Alikhodja, H.: Transboundary transport of non-east and East Asian dust observed at Dunhuang, northwest China, *Atmospheric Environment*, 318, 10.1016/j.atmosenv.2023.120197, 2024.
- Zhou, Y. and Wang, J.: The Composition and Assembly of Soil Microbial Communities Differ across Vegetation Cover Types of Urban Green Spaces, *Sustainability*, 15, 10.3390/su151713105, 2023.
- 590